4D Density Determination of NH Radicals in an MSE Microplasma Combining Planar Laser Induced Fluorescence and Cavity Ring-Down Spectroscopy

Martin Visser, Andreas Schenk and Karl-Heinz Gericke

Technische Universität Braunschweig, Institut für Physikalische und Theoretische Chemie
Hans-Sommer-Str. 10, 38106 Braunschweig, Germany

Abstract. An application of microplasmas is surface modification under mild conditions and of small, well defined areas. For this, an understanding of the plasma composition is of importance. First results of our work on the production and detection of NH radicals in a capacitively coupled radio frequency (RF) microplasma are presented. A microstructured comb electrode was used to generate a glow discharge in a hydrogen/nitrogen gas mixture by applying 13.56 MHz RF voltage. The techniques of planar laser induced fluorescence (PLIF) and cavity ring-down spectroscopy (CRDS) are used for space and time resolved, quantitative detection of the NH radical in the plasma. The rotational temperature was determined to be 820 K and, the density 5.1×10^{12} cm³. Also, time dependent behaviour of the NH production was observed.

Keywords: Microplasma, Free radicals, HF discharges, Microdischarges, Laser induced fluorescence (LIF), Non-thermal plasma, Radio frequency glow discharges (RFGD), Cavity ring-down spectroscopy (CRDS)
PACS: 52.25.Os, 52.27.Cm, 52.38.Dx, 52.50.Dg, 52.70.Kz, 52.80.Hc, 52.80.

INTRODUCTION

Microplasma sources have been drawing attention recently due to their small footprint and the unique plasma conditions. The small scale of the plasma permits operation at high pressures and low powers resulting in a non-thermal, "cold" plasma. These features, in conjunction with the progress in microfabrication, allow the integration of plasma sources into microsystems and their application in treatment of sensitive materials. Various types of microsources can be found in the literature spanning the full bandwidth of plasma generation, such as inductively coupled plasmas, dielectric barrier discharges and microwave excitation to name a few [1,2].

A field of particular interest in plasma research is the treatment and modification of surfaces [1,3], this, of course, is also the case in the field of microplasmas.

In this work we present some results of the study on a micro structured electrode (MSE) [4] RF powered plasma used for the generation of NH radicals, which are believed to play an important role in forming nitrogen containing functional groups (amino and nitrile) in the surface modification of hydrocarbon polymers. For applications, the spatial density distribution of the species in question may be of great importance. In our approach we use a combination of two spectroscopic techniques. The PLIF technique allows the temporal and spatial mapping of relative number densities. The second method used is CRDS, a sensitive absorption method providing absolute density measurement.

EXPERIMENTAL

Experimental Setup

The details of the LIF or PLIF technique [5,6] and of CRDS [7] can be found elsewhere, so only a brief introduction and a description of the setup will be given here.

Cavity Ring-Down Spectroscopy

Cavity ring-down spectroscopy is an absorption technique using a high finesse optical cavity usually made out of two highly reflective concave mirrors facing each other. Laser light is trapped between the two by irradiating the back of one of the mirrors, the "entrance mirror", which allows a small fraction of the

CP1282, *New Trend in Applied Plasma Science and Technology – ISAPS '09*
edited by A. Kobayashi, T. Miyasaka, and J. Krasa

laser light to enter the cavity. The light then travels back and forth in the cavity after the laser is switched off, gradually losing intensity either by passing through the mirrors or by any other loss mechanisms, one being absorption. The change in intensity in the cavity can be monitored by a detector behind the "exit mirror", as the intensity leaving the cavity is directly proportional to the intensity inside. It can be shown [7] that this change in intensity follows an exponential decay, and that its time constant is a direct measure of the losses of the cavity, intrinsic and introduced:

$$I_t = I_0 \cdot e^{-\left(\frac{1}{\tau}+\alpha c\right)t} = I_0 \cdot e^{-\frac{t}{\tau'}} \qquad (1)$$

In which I_t is the intensity of the light leaving the cavity at time t, I_0 is the initial intensity, τ is the time constant of the undisturbed cavity, α is the product of density N and absorption crosssection $\sigma(\lambda)$ of any species that might be present in the cavity, c is the speed of light and finally τ' represents the time constant which is actually measured and which equals the time constant of the undisturbed cavity in the case of zero absorption, neglecting losses other than absorption in this case.

Absorption may then be calculated using the slightly altered equation (1)

$$\frac{1}{\tau} + \sigma(\lambda)Nc = \frac{1}{\tau'} \qquad (2)$$

Furthermore, as the time constant and not the intensity is the value of interest, the method is intrinsically calibration free and partly immune to intensity fluctuations.

Planar Laser Induced Fluorescence

The difference of PLIF compared to common LIF is its added planar resolution which is introduced by using a laser sheet for excitation and detecting the light with 2D resolution rather than gathering all emitted light onto a single detector. As a result an image representing the fluorescence distribution in the probed (flat) volume is obtained. To convert this image to a density chart of the desired species two things need to be done, the correction of the fluorescence intensity due to the possible non-uniformity of the exciting laser sheet, and the calibration of the fluorescence intensity i.e. relating any part of the fluorescence image to the density at the same place.

The first may be done by acquiring a fluorescence image of a density distribution which is known to be uniform (bulk gas), which then represents the laser intensity distribution, and to divide by this reference the image with unknown density distribution. Care must be taken, though, as division by very small numbers, which might be present in the reference, could lead to infinitely large numbers in the resulting image. Intrinsically, a non-uniformity of a laser beam focused by a cylindrical lens should only be observable perpendicular to the direction of propagation, as its intensity decrease by absorption along the progation axis usually is negligibly small under most circumstances.

The second, relating the fluorescence intensity to a density, is in our case to be done measuring the average density along a given axis, ideally the optical path of the PLIF beam, by cavity ring down spectroscopy. The ratio of the average density and the integrated fluorescence intensity along this same axis then is the calibration factor allowing the intensity map to be converted to a density map.

In our experiments, the transition $A^3\Pi(v=0) \leftrightarrow X^3\Sigma^-(v=0)$ [8,9] of the NH-radical around 335 nm is used for both absorption and fluorescence measurements.

Experimental Procedure

In Figure 1 a scheme of our experimental setup is shown.

The MSE is mounted on a water-cooled heat sink which can be shifted vertically by a translation stage. This system is placed in a cylindrical vacuum chamber (25x40 cm) with flanges to admit power, cooling water and gas supply to the chamber through mass flow (MKS and Bronkhorst) and pressure controllers

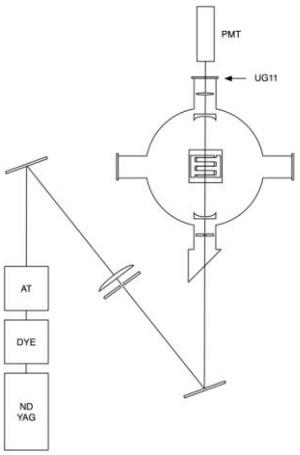

FIGURE 1. Top-view scheme of the experimental setup. Only the cylindrical lens outside the chamber together with the aperture inside the chamber are fitted for PLIF; the cavity mirrors, PMT, exit lens and the aperture outside the chamber only for CRDS. Supply lines and the camera (situated directly above the chamber, looking down) are left out for brevity.

(MKS) as well as optical access from the sides and a window insert in the lid to get a close top view with an ICCD camera (LaVision FlameStar II).

The MSE has a comb like structure, as outlined in Figure 1, and a total active area of 1x0.8 cm, details may be found in reference [4], it is driven by a 13.56 MHz radio frequency (RF) generator and associated impedance matchwork (ENI AGC 3b) through which 30 W of RF power are fed to the reactor, the back of the electrode is kept at 20°C by the heat sink and thermal compound. The plasma was ignited in an N_2/H_2 (50%/50%) atmosphere with a constant feed of fresh gas (20 sccm of each component). The total pressure was kept constant at 20 mbar *via* a pressure control valve connected to a rotary vane pump.

The laser system is used for both PLIF and CRDS. Its components are a pulsed dye laser (Radiant Dyes DL-midi, DCM in dimethylsulfoxide) tunable from 675 to 650 nm pumped by an Nd:YAG laser (Continuum Surelite, 10 Hz) at 532 nm. Frequency doubling is performed by a BBO crystal mounted inside an Inrad autotracker (AT) providing pulse energies around 100 μJ at 333 nm.

For PLIF measurements, the laser beam is passed through a cylindrical lens (f=1000 mm) and steered through the measuring chamber with the focused, flattened beam situated just above and parallel to the MSE exciting a broad area (in the x-y plane). To obtain only the well focused light, 12 cm away from the MSE a 5x1 mm aperture is placed, through which the beam has to pass. Spatial resolution in z direction is made possible by the translation stage as the distance can be adjusted in 10 μm steps. Detection of the fluorescence light is achieved by an ICCD camera equipped with a 50 mm f/1 lens and a 3 mm Schott type UG11 band pass filter to block visible and deep UV radiation emitted by the plasma itself. In this configuration the camera has a field of view of approximately 7.5x5 mm (576x384 pixels).

Some straightforward considerations need to be mentioned with respect to the timing of the laser/camera system in relation to the plasma. As the driving frequency of the plasma results in a period of 73.7 ns and the camera is operated at a shutter time of 5 ns, the laser/camera system needs to be synchronized to the RF voltage as the plasma may change its state corresponding to the phase of the voltage. In our setup, the RF voltage is probed by a digital storage oscilloscope (LeCroy WRXi 640). The oscilloscope then issues a trigger pulse at 10 Hz which is locked to the RF, this pulse in turn triggers the laser/camera through a DG 535 delay generator. Changing the timing of the camera and the laser with respect to the synchronization pulse therefore permits resolving the temporal behavior of the plasma in addition to the spatial resolution.

The images taken during an experiment are then processed by a home made computer program allowing integration of selected areas of each image which may then be plotted versus RF phase, laser wavelength or any spatial position, so full 4D resolution is achieved.

Cavity Ring-Down measurements were performed with the same laser system along the same optical axis as the PLIF experiments. For this, a small, central portion of the laser beam, gained by a 1 mm aperture, is steered into the chamber and focused into the optical cavity consisting of two plano-concave mirrors (R=200 mm, Layertec) with a centre wavelength of 330 nm. The cavity length is 22 cm and the ring-down time of the empty system has been measured in the range of interest and is around 850 ns which corresponds to a reflectivity of 99.91%. Inside the cavity two 1 mm apertures were placed close to the mirrors to enhance spatial resolution. Behind the exit mirror of the cavity a lens is placed focusing the exiting light through a UG 11 band pass Filter (see above) onto the detector. For detection, a photomultiplier tube (PMT) type R1617 (Hamamatsu) was used which was directly connected to the oscilloscope for data acquisition and processing.

The MSE is situated in the middle of the cavity and lifted up as close to the optical path as possible without disturbing the ring-down trace *via* the translation stage.

RESULTS AND DISCUSSION

Results

Figure 2 shows the spectrum of NH recorded using PLIF and CRDS under the conditions mentioned above. In both cases the measurement was conducted

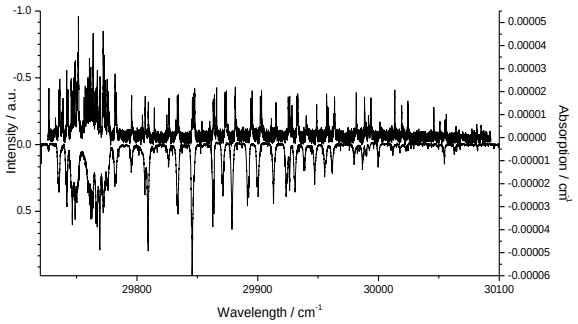

FIGURE 2. Part of the NH spectrum recorded in the $A^3\Pi(v=0)\leftrightarrow X^3\Sigma\text{-}(v=0)$ band. Top: CRD spectrum, scale on the right. Bottom, inverted: PLIF spectrum, scale on left.

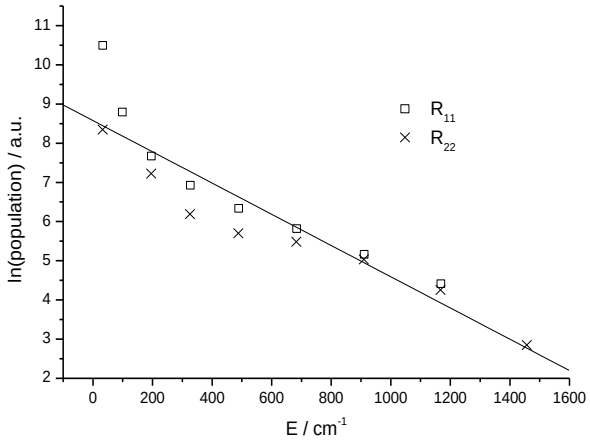

FIGURE 3. Boltzmann plot for temperature determination and verification of rotational equilibrium. The straight line represents the linear fit of the data, resulting in a temperature of 820 K.

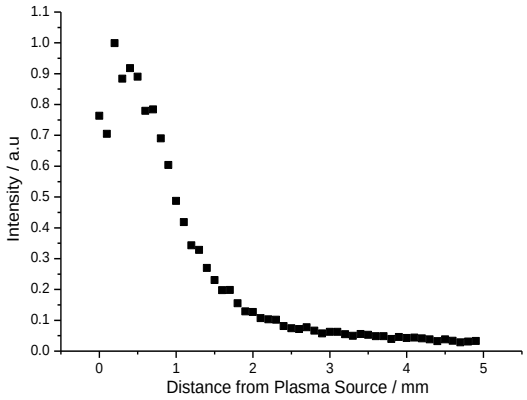

FIGURE 4. Vertical change in fluorescence.

as close as possible to the MSE surface, i.e. ~0.6 mm from MSE surface to the beam centre. The CRDS spectrum was obtained by recording five ring-down events for each wavelength which were then fitted individually using a non-linear least squares fitting algorithm and subsequent averaging. The PLIF spectrum was recorded in portions and then stitched together, no correction was made for variations in laser intensity which accounts for differences comparing PLIF and CRDS data. The spectra compare well with data by Brazier and Lents [8,9] confirming the presence of NH.

An estimate of the absolute density of NH radicals is difficult due to the complicated determination of the absorption cross section, but was made according to the procedure of van den Oever et al. [10].

The rotational temperature was determined by a Boltzmann plot, depicted in Figure 3. Using the R_{11} and R_{22} branches from J=2 to 10 and J=1 to 9, respectively, it was calculated to be 820 K. This in course also shows the NH radicals are in rotational equilibrium slightly above the MSE plane.

Using the $R_{11}(2)$ absorption line at 29809.82 cm^{-1} and taking into account the temperature mentioned above, the resultant number density is 5.1×10^{12} cm^3

Spectroscopic constants were obtained from Refs [8,9]. The absorption length was 8 mm of the 22 cm of the cavity length.

The dimensions of the NH containing area of the plasma including absorption length can be determined from a camera image such as Figure 5b. Below the plot two original camera images are shown. The right image shows the induced fluorescence together with the plasma running, the left one shows the plasma alone. One of the two comb-like sets of electrodes of the MSE can be recognized in this image by its glow. The vertical stripes therefore have a breadth of 1.6 and 0.8 mm and may be used as a measure. As the intensity drops sharply at the edges of the MSE the absorption path length used for the CRDS measurement is estimated to be the same as the width of the MSE, i.e. 8 mm.

In height, the NH containing volume of the plasma can be estimated from Figure 4. The plot shows the NH fluorescence intensity with the laser passing at different heights above the plasma. The ordinate specifies the traveled distance of the translation stage moving the MSE away from the laser beam. At minimum distance the beam still hits the edge of the MSE, so the fluorescence maximum is observed at a traveled distance of 0.6 mm. It may be assumed, that at this setting the beam is passing over the MSE at its full vertical diameter of 1 mm. After this, the plot exhibits a fast drop of intensity showing the very small volume of the NH production.

Time resolution is achieved by the PLIF portion of the experiment. The laser beam exciting the radicals has a pulse duration of well less than 5 ns and the camera a minimum exposure time of 5 ns compared to the 74 ns needed for one full cycle of the RF generator voltage. In Figure 5 four sets of data are plotted versus the period T of the plasma generator: The intensity of the plasma glow alone over each of the electrodes and the intensity of NH fluorescence in the running plasma over the same areas. Clearly, time dependent behavior is observed which also shows a slight difference for each electrode. The fluorescence shows a steady increase over both electrodes for about half a period and then stays almost constant for another half period. After that a sharp drop occurs and the scheme repeats.

a

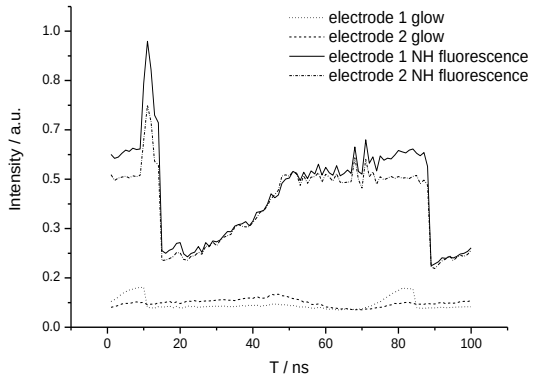

b

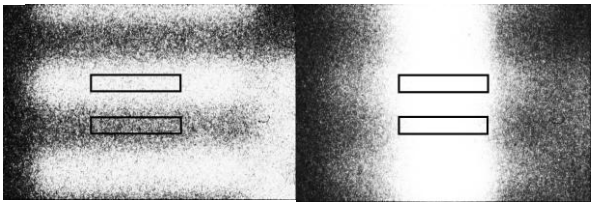

FIGURE 5. a) top, Time resolved plasma glow and fluorescence recorded over each of the two electrodes.
b) bottom, left: plasma glow, right: plasma glow and NH fluorescence. The rectangles mark the observed areas.

The glow alone only shows small variations, but a significant difference between the two electrodes. Electrode 1 shows a short increase to almost double intensity before it drops to normal again, while electrode 2 undergoes only small and less marked changes. This occurs synchronously to the patterns in fluorescence plots, slightly shifted to shorter times. These data suggest that the two electrodes are not working symmetrically with respect to the phase of the RF generator. In the symmetric case, fluorescence and glow should show a similar pattern over each electrode repeating itself every full period as both electrodes should work identically with a phase difference of 180°.

Looking at both electrodes together one would expect a resultant with a repetition rate of a half-period, clearly, this is not the case. All four patterns observed do repeat themselves each full period, but seem to be "in phase" so in sum no half-period pattern is obtained.

CONCLUSION

It has been shown that using a MSE

(1) an NH producing plasma is obtained at reduced pressures and
(2) the radical distribution in the discharge area is monitored with spatial resolution applying the PLIF method.
(3) Cavity ring-down spectroscopy which is used for calibration of the fluorescence data is applicable under the conditions given.
(4) The rotational temperature of the NH radicals was estimated at 820 K. Using the approach of Luque et al. [6] the absolute values of NH concentration are to be used to calibrate the PLIF data.
(5) The usefulness of PLIF for studies of the temporal behaviour of the plasma source has been shown and as a result the non-symmetric behavior of the plasma in time was observed.

ACKNOWLEDGEMENTS

The authors would like to thank the Deutsche Forschungsgemeinschaft and the Braunschweig International Graduate School of Metrology.

REFERENCES

1. U. Kogelschatz, *Contrib. Plasma Phys*., **47**-1, 80-88 (2007).
2. K. Tachibana, *IEEJ Transactions on Electrical and Electronic Engineering*, **1**-2, 145-155 (2006).
3. J. Meichsner, *Low Temperature Plasmas (2nd Edition)* 2, Wiley-VCH, Weinheim, Germany, 2008, pp.739-756.
4. L. Baars-Hibbe, P. Sichler, C. Schrader, C. Geßner, K.-H. Gericke, S. Büttgenbach, *Surf. Coat. Technol.*, **174**, 519-523 (2003).
5. I. van Cruyningen, A. Lozano, R. K. Hanson, *Exp. Fluids*, **10**, 41-49 (1990).
6. J. Luque, J.B. Jeffries, G.P. Smith, D.R. Crosley, *Appl. Phys. B*, **73**, 731-738 (1990).
7. A. OKeefe, D.A.G. Deacon, *Rev. Sci. Instrum*., **69**, 2544 (1998).
8. C. R. Brazier, R.S.Ram, P.F.Bernath, *J. Mol. Spectr*., **120**, 381-402 (1986).
9. J. M. Lents, *J. Quant. Spectr. Rad. Trans*., **13**, 297-310 (1973).
10. P. J. van den Oever, J. H. van Helden, C. C. H. Lamers, R. Engeln, D. C. Schram, M. C. M. van de Sanden, W. M. M. Kessels, *J. Appl. Phys*., **98**, 093301 (2005).